Two-dimensional Fluid Simulation of an RF Capacitively Coupled Ar/H_2 Discharge

Lizhu Tong[1]
[1]Keisoku Engineering System Co., Ltd.
1-9-5 Uchikanda, Chiyoda-ku, Tokyo 101-0047, Japan, tong@kesco.co.jp

Abstract: The capacitively coupled radio-frequency (RF) discharges in Ar/H_2 mixtures are investigated by a two-dimensional fluid model in this work. The discharge properties in a mixture of Ar with 1%H_2 operating at a RF frequency of 13.56 MHz are simulated and compared with those of the pure Ar, in which a blocking capacitor of 0.1 μF is serially connected to the power electrode. The density profiles of all the chemical species in the plasma are obtained. The self dc bias generated by the blocking capacitor is estimated. Results show that with the addition of small amount of H_2 to Ar, the electron density markedly decreases. A large potential difference is found to occur at the surface area between the substrate and focus ring, in which the high power deposition is presented.

Keywords: Ar/H_2 mixture, CCP plasma, Blocking capacitor, self DC bias.

1. Introduction

Ar/H_2 discharges are frequently used in various industrial applications, such as etching processes, surface treatment, and film deposition [1-5]. An overview of the possible reactions in an Ar/H_2 discharge has been reported [6]. In the discharges, the active species, such as ions and hydrogen atoms, are responsible for surface reactions, which could be considered as the most important parameters in the study of Ar/H_2 plasmas [7]. The simulation method will no doubt be an efficient tool to obtain these parameters.

Capacitively coupled radio-frequency (RF) discharges are among the most powerful and flexible plasma reactors, widely used both in research and in industry [8]. The particle-in-cell/Monte Carlo (PIC-MC) model has been developed to study the properties of 1D RF capacitively coupled plasmas (CCPs) [9] and 2D DC glow discharges [10] in Ar/H_2. It has been indicated [11] that although for the regime of operation a kinetic description based on the particle scheme can provide accurate electron energy distribution, the fluid approximation can be applicable in low pressure plasma discharges. Moreover, since the simulation of CCPs based on the particle scheme is very computationally intensive, a two-dimensional fluid model is taken into account in the present research. The numerical solution is performed using the Plasma Module of COMSOL Multiphysics 4.4. The discharge properties of the Ar/H_2 CCP plasmas are obtained and the effects of focus ring and blocking capacitor are presented.

2. Numerical Model

The model geometry used in this work is shown in Fig. 1, which has been described in earlier literatures [12,13]. An RF source is connected to the bottom electrode (metal substrate) through a blocking capacitor of 0.1 μF and is surrounded by focus ring and dielectric. The top electrode and side metal are grounded. The inter-electrode gap is 3.2 cm.

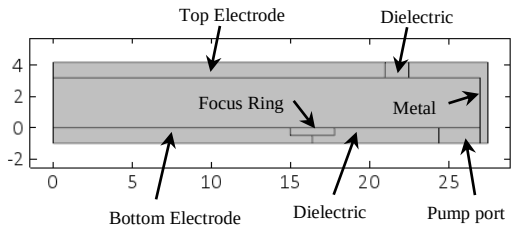

Figure 1. Model geometry used in this work.

The simulations are performed for the case of $Ar/1\%H_2$ CCP plasma discharges operating at a RF frequency of 13.56 MHz. The RF-applied voltage is 200 V. The gas pressure is 100 Pa and the gas temperature is assumed to be 300 K. The species taken into account are electrons, molecules (Ar, H_2), ions (Ar^+, H^+, H_2^+, H_3^+, ArH^+), and neutrals (Ar^*, H, H(2*p*), H(2*s*)). The reactions of electron impact collision and those of ions and neutral species are listed in Table 1.

The basic equations for the plasma simulation used in this research include a pair of drift diffusion equations for the electrons, a modified Maxwell–Stefan equation for the ion and neutral

species, and a Possion's equation for the space charge electric field. The detailed information for the model can be found in our previous work [11]. In this work, the charge accumulation on the dielectric surface is modelled

$$\mathbf{n} \cdot (\mathbf{D}_1 - \mathbf{D}_2) = \rho_s, \quad (1)$$

where ρ_s is the solution of the following equation on the dielectric surface

Table 1: The reactions included in the model.

No.	Reaction	Ref.
1	$Ar + e^- \rightarrow Ar + e^-$	14,15
2	$Ar + e^- \rightarrow Ar^* + e^-$	14,15
3	$Ar + e^- \rightarrow Ar^+ + 2e^-$	14,15
4	$Ar^* + e^- \rightarrow Ar^+ + 2e^-$	14,15
5	$Ar^* + Ar^* \rightarrow Ar^+ + Ar + e^-$	14,15
6	$Ar^* + Ar \rightarrow Ar + Ar$	14,15
7	$H_2 + e^- \rightarrow H_2 + e^-$	16
8	$H_2 + e^- \rightarrow H + H + e^-$	7
9	$H_2 + e^- \rightarrow H + H(2s) + e^-$	7
10	$H_2 + e^- \rightarrow H(2p) + H(2s) + e^-$	7
11	$H_2 + e^- \rightarrow H_2^+ + 2e^-$	7
12	$H_2 + e^- \rightarrow H + H^+ + 2e^-$	7
13	$H_2^+ + e^- \rightarrow H^+ + H + e^-$	7
14	$H_3^+ + e^- \rightarrow H_2 + H$	7
15	$H_2 + H_2^+ \rightarrow H_3^+ + H$	7
16	$H + e^- \rightarrow H + e^-$	16
17	$H + e^- \rightarrow H(2p) + e^-$	7
18	$H + e^- \rightarrow H(2s) + e^-$	7
19	$H(2s) + e^- \rightarrow H(2p) + e^-$	7
20	$H + e^- \rightarrow H^+ + 2e^-$	7
21	$H(2s) + e^- \rightarrow H^+ + 2e^-$	7
22	$H(2p) \rightarrow H + hv$	7
23	$Ar^* + H_2 \rightarrow Ar + H + H$	7
24	$Ar^+ + H_2 \rightarrow Ar + H_2^+$	7
25	$Ar^+ + H_2 \rightarrow H + ArH^+$	7
26	$ArH^+ + H_2 \rightarrow H_3^+ + Ar$	7
27	$ArH^+ + e^- \rightarrow Ar + H$	7
28	$Ar^* \rightarrow Ar$ (wall loss)	14
29	$H_2^+ \rightarrow H_2$ (wall loss)	14,7
30	$H_3^+ \rightarrow H + H_2$ (wall loss)	14,7
31	$H^+ \rightarrow H$ (wall loss)	14,7
32	$H \rightarrow 1/2H_2$ (wall loss)	14,7
33	$H(2p) \rightarrow H$ (wall loss)	14
34	$H(2s) \rightarrow H$ (wall loss)	14,7

$$d\rho_s/dt = \mathbf{n} \cdot \mathbf{J}_i + \mathbf{n} \cdot \mathbf{J}_e, \quad (2)$$

where $\mathbf{n} \cdot \mathbf{J}_i$ is the normal component of the total ion current density on the dielectric surface and $\mathbf{n} \cdot \mathbf{J}_e$ is the normal component of the total electron current density on the dielectric surface.

In plasma simulations, the initial electron number density is assumed to be 1×10^{13} m^{-3} and initial electron energy is 4 eV. For the initial ion number densities, H^+, H_2^+, H_3^+, ArH^+ ions are assumed to be 1×10^{11} m^{-3} and Ar^+ is assigned by sustaining the electroneutrality. The secondary electron emission due to ion impact is set to zero and ions are considered as completely absorbed/ neutralized when they arrive at the electrodes. The excited hydrogen atoms and argons are set to revert to their ground states when they contact with the walls. The surface loss of hydrogen atoms is given [11]

$$R = -\left(\frac{\gamma}{1-\gamma/2}\right)\frac{v}{4}c, \quad (3)$$

where c is the density of hydrogen atom, $v = \sqrt{8k_BT/\pi m}$ is the average velocity of the hydrogen atoms, where k_B is the Boltzmann constant, T is the temperature, and m is the mass of hydrogen atom. γ is the surface loss probability, which is assumed to be 0.07 in this work [7,11].

3. Simulation results

3.1 Discharge structure

Figure 2 shows the calculation results for an Ar/1%H_2 CCP plasma. The maximum of electron densities arrives at 1.26×10^{16} m^{-3}, distributed above the focus ring. The high electron temperature regions appears in the neighborhood of electrodes, with a maximum value of 28.1 eV. The Ar^+, ArH^+ and H_3^+ ions are the dominant ions in the plasma, which is consistent with the previous research [4,10]. It is known that a high hydrogen dissociation rate as sources of hydrogen atoms is required in hydrogen containing discharges [7]. In the present research, a high hydrogen dissociation rate over 1×10^{20} m^{-3}s^{-1} in the plasma center causes the hydrogen atom density increase up to the maximum of 2.31×10^{17} m^{-3}, being about 20 times of the electron density.

Results show a large potential difference occurred at the surface area between the substrate and focus ring. The local power deposition at t = T/4 is shown in Fig. 2, in which T is the RF period.

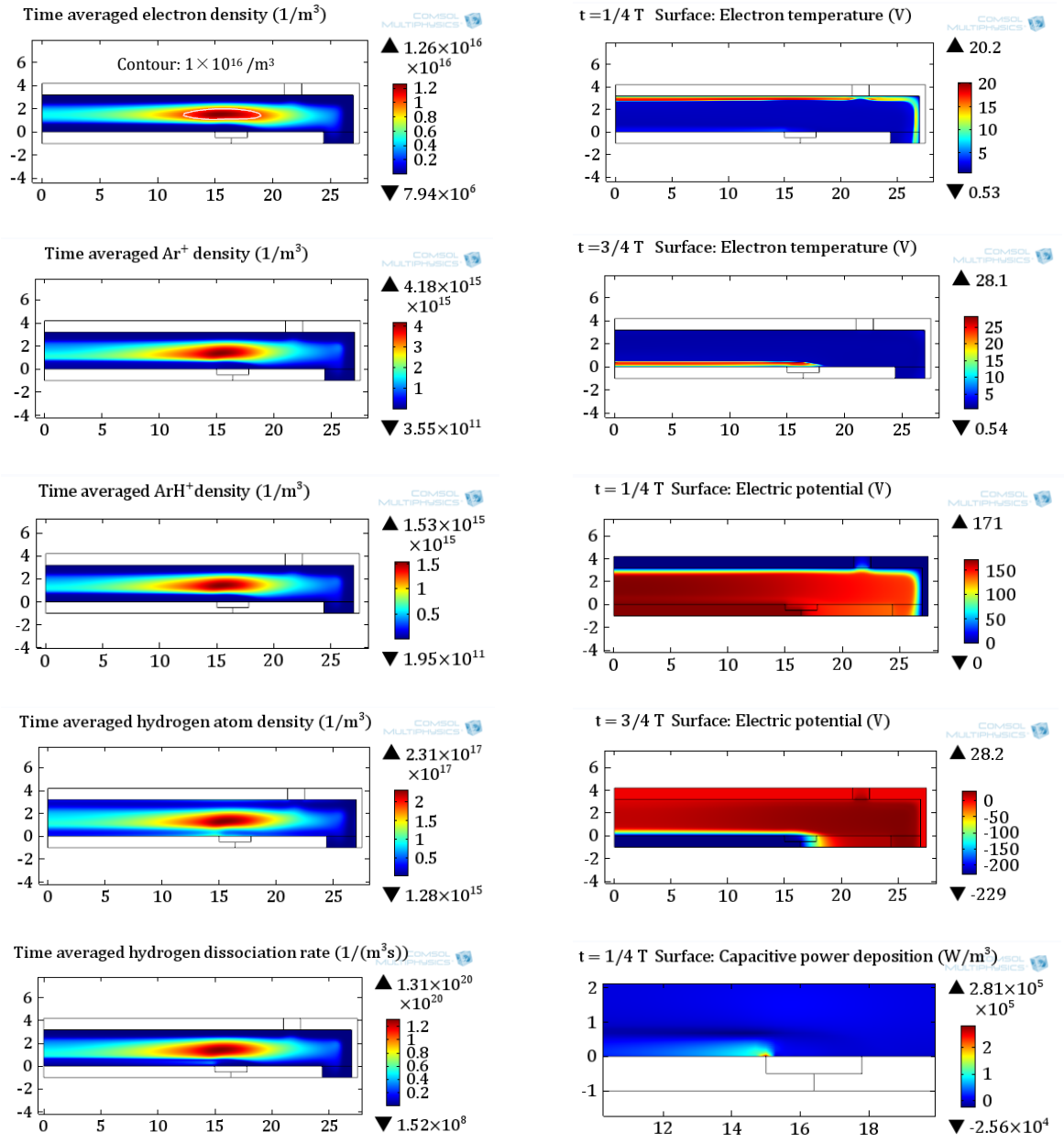

Figure 2. CCP Discharge structure for the Ar/H_2 mixture (Ar/H_2 = 99/1, V_{rf} = 200 V, *RF* = 13.56 MHz, *p* = 100 Pa, C_b = 0.1 μF, and *T* is the RF period).

The local high power deposition demonstrates the effect of the potential difference between the substrate and focus ring. This could become a main reason that the highest electron density region is concentrated around the focus ring, not being in the center of the reactor, as shown by the contour of 1×10^{16} m^{-3} of electron density in Fig. 2.

3.2 Effect of the blocking capacitor

The use of a blocking capacitor is known to generate a self DC-bias in CCP plasmas [17]. Figure 3 show the difference between the calculated electric potential on the substrate and the RF-applied voltage, which is regarded as the

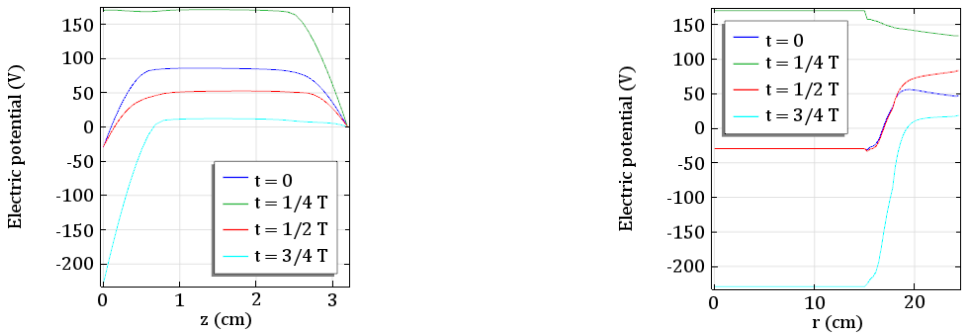

Figure 3. Electric potential at the axis of the reactor and along the surface of substrate and adjacent dielectrics in the Ar/H_2 CCP (Ar/H_2 = 99/1, V_{rf} = 200 V, *RF* = 13.56 MHz, *p* = 100 Pa, C_b = 0.1 μF, and *T* is the RF period).

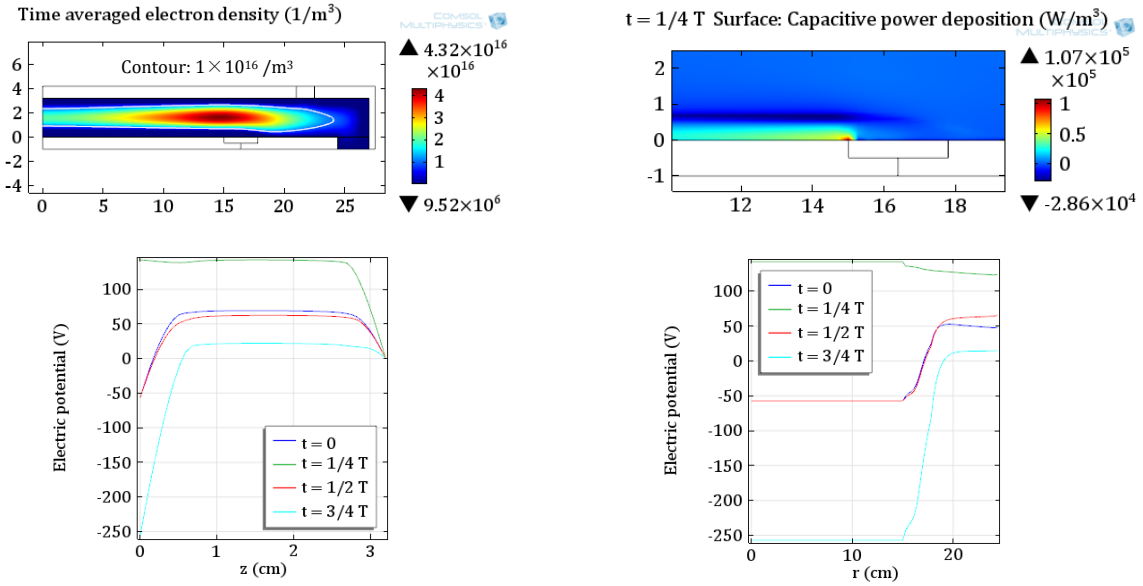

Figure 4. Electron density, power deposition and electric potential at the axis of the reactor and along the surface of substrate and adjacent dielectrics in the pure Ar CCP (V_{rf} = 200 V, *RF* = 13.56 MHz, *p* = 100 Pa, C_b = 0.1 μF, and *T* is the RF period).

self DC-bias. During a RF period, the self DC-bias slightly varies between -29 and -30 V.

3.3 Comparison with the discharge of pure argon

Figure 4 shows the calculated results for a pure Ar CCP plasma. The computational conditions are set the same as the above-described Ar/1%H_2 model. The electron density in the pure Ar is much higher than that of Ar/1%H_2 model, in which the maximum electron density arrives at 4.32×10^{16} m^{-3}. The contour of 1×10^{16} m^{-3} of electron density appears a wide range in the center of the reactor, which is much larger than that of Ar/1%H_2 model, as shown in Fig. 2. A large potential difference is also found at the surface area between the substrate and focus ring. The corresponding local power deposition at t = T/4 is shown in Fig. 4. The effect of the blocking capacitor for the pure Ar presents a larger self DC-bias, possessed of an estimated value of -58 V. The higher plasma density could be considered as a reason to generate a higher self DC-bias.

4. Conclusions

This paper presents the simulation results of low-pressure capacitively coupled RF plasmas in Ar/H_2. The calculation is performed by COMSOL Multiphysics. It is found that the addition of small amount of H_2 to Ar cause the electron density markedly decrease. The high electron density region is formed above the focus ring. The effect of the self DC-bias of the blocking capacitor is demonstrated. It could be concluded that the control of the focus ring and blocking capacitor would be very beneficial in finding the design parameters of RF CCP plasma reactors.

5. References

1. H.C. Barshilia, A. Ananth, J. Khan, G. Srinivas, "$Ar+H_2$ plasma etching for improved adhesion of PVD coatings on steel substrates", *Vacuum*, **86**, 1165-1173 (2012)

2. A. Kahouli, A. Sylvestre, J-F. Laithier, S. Pairis, J-L. Garden, E. André, F. Jomni, B. Yangui, "Effect of O_2, Ar/H_2 and CF_4 plasma treatments on the structural and dielectric properties of parylene-C thin films", *J. Phys. D: Appl. Phys.*, **45**, 215306 (2012)

3. Z. Tang, W. Wang, D. Wang, D. Liu, Q. Liu, D. He, "The influence of H_2/Ar ratio on Ge content of the μc-SiGe: H films deposited by PECVD", *J. Alloy Compd.*, **504**, 403-406 (2010)

4. J. Umetsu, K. Koga, K. Inoue, H. Matsuzaki, K. Takenaka, M. Shiratani, "Discharge power dependence of H_α intensity and electron density of $Ar+H_2$ discharges in H-assisted plasma CVD reactor", *Surf. Coat. Technol.*, **202**, 5659-5662 (2008)

5. K. Ostrikov, H-J. Yoon, A.E. Rider, V. Ligatchev, "Reactive species in $Ar+H_2$ plasma-aided nanofabrication:two-dimensional discharge modelling", *Phys. Scr.*, **76**, 187-195 (2007).

6. A. Bogaerts, R. Gijbels, "Effects of adding hydrogen to an argon glow discharge: overview of relevant processes and some qualitative explanations", *J. Anal. At. Spectrom.*, **15**, 441-449 (2000)

7. T. Kimura, H. Kasugai, "Properties of inductively coupled rf Ar/H_2 plasmas: Experiment and global model", *J. Appl. Phys.*, **107**, 083308 (2010)

8. L.L. Alves, L. Marques, "Fluid modelling of capacitively coupled radio-frequency discharges: a review", *Plasma Phys. Control. Fusion*, **54**, 124012 (2012)

9. E. Neyts, M. Yan, A. Bogaerts, R. Gijbels, "PIC-MC simulation of an RF capacitively coupled Ar/H_2 discharge", *Nucl. Instr. Meth. Phys. Res.* B, **202**, 300-304 (2003)

10. A. Bogaerts, R. Gijbels, "Hybrid Monte Carlo-fluid modeling network for an argon/ hydrogen direct current glow discharge", *Spectrochim. Acta Part B*, **57**, 1071-1099 (2002)

11. L.Z. Tong, "Study of low pressure inductively coupled plasmas: Effects of the DC bias and gas flow rate", *Jpn. J. Appl. Phys.*, **52**, 05EA03 (2013)

12. A. Agarwal, S. Rauf, K. Collins, "Gas heating mechanisms in capacitively coupled plasmas", *Plasma Sources Sci. Technol.*, **21**, 055012 (2012)

13. S. Rauf, K. Bera, K. Collins, "Self-consistent simulation of very high frequency capacitively coupled plasmas", *Plasma Sources Sci. Technol.*, **17**, 035003 (2008)

14. COMSOL Multiphysics 4.4 - Plasma Module Library Models and also http://www.comsol.com

15. D.P. Lymberopoulos, D.J. Economou, "Fluid simulations of glow discharges: Effect of metastable atoms in argon", *J. Appl. Phys.*, **73** (8) 3668-3679 (1993)

16. J.L. Giuliani, V.A. Shamanian, R.E. Thomas, J.P. Apruzese, M. Mulbrandon, R.A. Rudder, R.C. Hendry, A.E. Robson, "Two-dimensional model of a large area, inductively coupled, rectangular plasma source for chemical vapor deposition", *IEEE Trans. Plasma Sci.*,**27**(5),1317-1328 (1999)

17. S. Song, M.J. Kushner, "Role of the blocking capacitor in control of ion energy distributions in pulsed capacitively coupled plasmas sustained in $Ar/CF_4/O_2$", *J. Vac. Sci. Technol. A*, **32**(2),021306 (2014)